Materials Advances

ROYAL SOCIETY OF CHEMISTRY

PAPER

View Article Online
View Journal | View Issue

Cite this: *Mater. Adv.*, 2025, 6, 2636

A chia (*Salvia hispanica* L.) seed mucilage-based glucoxylan-grafted-acrylic acid hydrogel: a smart material for pH-responsive drug delivery systems

Maria Khatoon,[a] Arshad Ali,[a] Muhammad Ajaz Hussain, *[b] Muhammad Tahir Haseeb,[c] Gulzar Muhammad,[d] Muhammad Sher,[a] Syed Zajif Hussain,[e] Irshad Hussain[e] and Munawar Iqbal[b]

The present research study is based on the extraction of the chia seed mucilage (CSM) composed of a polysaccharide (glucoxylan). The CSM and acidic monomer acrylic acid (AA) are used to synthesize a copolymer hydrogel, *i.e.*, CSM-grafted-polyacrylic acid (CSM-*g*-PAA), as a novel pH-dependent sustained release drug delivery system (DDS). Fourier transform infrared (FTIR) spectroscopy and solid-state cross-polarization magic angle spinning nuclear magnetic resonance (CP/MAS ^{13}C NMR) spectroscopy analyses confirmed the formation of CSM-*g*-PAA through the graft copolymerization of the CSM with AA. Scanning electron microscopy (SEM) images demonstrated the porous surface of CSM-*g*-PAA. The swelling capacity (g g^{-1}) of CSM-*g*-PAA and drug (nicorandil) release (%) from nicorandil-loaded CSM-*g*-PAA (Nic-CSM-*g*-PAA) were found to be dependent on the pH of the dissolution medium and the concentrations of CSM, AA, and the crosslinker *N*,*N*-methylene-bis-acrylamide (MBA). The gel fraction (%) in CSM-*g*-PAA was increased upon increasing the concentrations of CSM, AA, and MBA. The porosity (%) of CSM-*g*-PAA was increased with the increase of CSM and AA concentrations and decreased with increasing MBA concentration. The drug was loaded onto CSM-*g*-PAA and the amount of nicorandil loaded onto CSM-*g*-PAA (mg g^{-1}) was determined by a gravimetric method. The loading amount of nicorandil onto CSM-*g*-PAA was found to be directly dependent on the swelling capacity of CSM-*g*-PAA. The swelling of CSM-*g*-PAA followed second-order kinetics, whereas nicorandil release at pH 6.8 and 7.4 from Nic-CSM-*g*-PAA followed first-order-kinetics. The mechanism of nicorandil release from Nic-CSM-*g*-PAA was non-Fickian transport. Conclusively, CSM-*g*-PAA could be an efficient vehicle for the targeted administration of nicorandil to the small intestine.

Received 17th January 2025,
Accepted 13th March 2025

DOI: 10.1039/d5ma00046g

rsc.li/materials-advances

1. Introduction

Naturally occurring polysaccharide-based mucilages isolated from plant seeds have been widely used in food processing, tissue engineering, biofilms, pharmaceutics, and nanomedicines.[1,2] Because of their distinctive physicochemical and biomechanical properties, polysaccharides/mucilages/hydrogels are considered as sustainable materials for drug delivery systems (DDSs) and many other biomedical applications with and without chemical modification.[3–8] *Salvia hispanica* L. (chia) is a plant of the *Lamiaceae* (mint) family. The chia plant has been cultivated as a crop in Mexico, northern Guatemala, Australia, Argentina, America, Bolivia, Colombia, Europe, and Peru.[9] The chia seeds are used to control diabetes and cardiovascular diseases.[10]

The mucilage of chia seeds (CSM) is a hetero-polysaccharide mainly composed of D-xylose, D-glucose, and glucuronic acid residues in the ratio of 2 : 1 : 1, respectively.[11] In a study, the CSM was purified through gel filtration and thoroughly characterized. Hydrolysis of the CSM revealed the presence of β-D-xylose, α-D-glucose, and 4-*O*-methyl-α-D-glucuronic acid. Structurally, the CSM consists of a linear tetrasaccharide backbone composed of aldobiouronic acid residues, specifically two D-xylopyranosyl units, one D-glucopyranosyl unit, and branches of 4-*O*-methyl-D-glucopyranosyluronic acid. This study showed that the CSM backbone is formed by repeating units of (1→4)-β-D-xylopyranosyl-(1→4)-α-D-glucopyranosyl-(1→4)-β-D-xylopyranosyl. Some β-D-xylopyranosyl residues in this backbone are substituted at *O*-2 with 4-*O*-methyl-α-D-glucuronopyranosyl branches. The structural composition of the CSM suggested a complex, branched polysaccharide structure with both linear

[a] *Institute of Chemistry, University of Sargodha, Sargodha 40100, Pakistan*
[b] *School of Chemistry, University of the Punjab, Lahore 54590, Pakistan. E-mail: majaz172@yahoo.com; Tel: +92 3468614959*
[c] *College of Pharmacy, University of Sargodha, Sargodha 40100, Pakistan*
[d] *Department of Chemistry, Government College University Lahore, Lahore 54000, Pakistan*
[e] *Department of Chemistry, SBA School of Science & Engineering, Lahore University of Management Sciences, Lahore Cantt, 54792, Pakistan*

and branched segments.[12] Based on these studies, it is revealed that the CSM consists of glucoxylan as a major polysaccharide.

The CSM has been utilized as a supplement to different bakery items (biscuits, cakes, cereals, pasta, and snacks),[13,14] an adhesive, a binder, an emulsifier, a suspending agent, foam, and an ice cream stabilizer to modify texture and viscosity.[15–18] The CSM acted as a plasticizer during film preparation and an excipient for drug delivery applications.[19]

The CSM is hydrophilic and chemically modifiable due to hydrophilic functionalities, *i.e.*, hydroxyl (–OH), carboxylic (–COOH), amino ($–NH_2$), *etc.* Carboxylic acid (–COOH) group containing monomers, such as acrylic acid (AA), are the most selective candidates to develop a pH-sensitive polymeric matrix for sustained delivery of hydrophilic drugs. The pH-sensitivity of AA-based hydrogels increased with pH due to pendant –COOH groups. The AA-based hydrogels offered low swelling at acidic pH and high swelling at alkaline pH. Therefore, once the drug is loaded onto AA-based hydrogels, they offer a higher release at alkaline pH due to deprotonation of –COOH groups and a lower release at acidic pH due to protonation of –COOH groups. Moreover, AA is a bio-degradable, biocompatible, bio-adhesive, and anti-bacterial material with a short elimination half-life, and hence, it has the potential for bioaccumulation.[20]

Hydrophilic drugs due to high water solubility are completely metabolized and rapidly eliminated, resulting in a short elimination half-life requiring frequent dosing. Such types of drugs require a sustained-release DDS.[21] The most common cardiovascular diseases (hypertension and angina pectoris) need regular intensive care. The most important class of drugs for this issue are potassium channel openers. One of the members of this class is nicorandil, which hyperpolarizes smooth muscle cell membranes and acts as a potent coronary vasodilator. Although nicorandil acts as one of the emerging molecules in the case of hypertension and angina, there is a problem with keeping its supply constant and uniform for maintaining blood pressure at a normal physiological level due to its short half-life.[22]

To reduce the frequency of administration and improve patient compliance, a once-daily sustained-release formulation of nicorandil is required. Therefore, the synthesis of a copolymer hydrogel, *i.e.*, CSM-*g*-PAA, based on the CSM and AA is reported herein for the first time. This study aims to synthesize an efficient novel matrix for pH-dependent and intelligent drug delivery by combining the CSM and AA through free radical polymerization. The structural and functional properties of CSM-*g*-PAA will be evaluated spectroscopically, *i.e.*, through FTIR, solid-state CP/MAS ^{13}C NMR, and SEM analyses. The concentrations of CSM, AA, and MBA will be varied to study their influence on the swelling capacity, porosity, sol–gel fraction, nicorandil loading, nicorandil release, and nicorandil release kinetics.

2. Materials and methods

2.1. Materials

Chia seeds were acquired from the local market of District Sargodha, Pakistan. A botanist at the Department of Biological Sciences, University of Sargodha, Pakistan verified the seed's taxonomy. The chia seeds were manually cleaned, sieved, and stored in air-tight jars at room temperature. The reagents and chemicals used in this research were highly pure and of analytical grade. Potassium dihydrogen phosphate (KH_2PO_4 (>99.97%)), NaOH (>99.97%), HCl (>99.97%), *n*-hexane (>99.97%), acetone (>99.97%), chloroform (>99.97%), methanol (>99.97%), and ethanol (>99.97%) were obtained from Sigma-Aldrich, USA. Acrylic acid (AA (>99.97%)) was obtained from Fischer Scientific, USA. Potassium persulfate (KPS (>99.97%)) and *N*,*N*-methylene-bis-acrylamide (MBA (>99.97%)) were purchased from Merck, Germany. The protocol as described in the United States Pharmacopeia (USP 34-NP 29) was used for the preparation of buffers (pH 1.2 and 7.4). Nicorandil (United States Pharmacopeia (USP)) was used as a standard drug. A nylon mesh sieve was used to isolate the CSM. All the glassware was initially rinsed with HNO_3 and then washed with distilled water (DW). DW was also used for the preparation of necessary solutions and dilutions.

2.2. Measurements

Samples (CSM and CSM-*g*-PAA) were accurately weighed and milled before converting them into disc-shaped pellets using KBr and a hydraulic press. The pellets obtained were dried in a vacuum oven before analysis. FTIR spectra of each sample were captured on an IRPrestige-20 spectrophotometer (Shimadzu, Japan) in the wavenumber range from 4000 to 400 cm^{-1}. The solid-state CP/MAS $^{13}CNMR$ (Bruker DRX-400 machine) spectrum of CSM-*g*-PAA was recorded to observe the sugar pattern. From the results of both of these analyses, the success of the polymerization reaction between CSM and AA was evaluated. The SEM (Nova, NanoSEM 450 machine) images of CSM-*g*-PAA were captured to monitor its surface morphology. CSM-*g*-PAA was swelled in the buffer of pH 7.4 and then sonicated for 15 min to remove the entrapped air bubbles and then freeze-dried. The freeze-dried sample was cut using a sharp blade and the transverse and longitudinal cross-sections were obtained. After that, the freeze-dried cross-sections of each sample were coated with gold using a sputter coater (Denton, Desk V HP). Finally, the SEM images of each sample were captured at 50, 100, and 300 nm. Moreover, the pore size was measured from the histograms of each sample.

2.3. Extraction of chia seed mucilage

Chia seeds (cleaned) were imbibed in DW for 12 h and then heated at 60 °C for 1 h. The mucilage extruded from swollen chia seeds was separated using nylon mesh. The mucilage (CSM) was purified by frequent washing with DW and *n*-hexane to remove polar and non-polar impurities, respectively. After purification, the CSM was spread on a steel tray for drying in an oven at 80 °C under vacuum and shade.[23] The dried CSM was stored in an air-tight container for further experimental work.

2.4. Synthesis of CSM-*g*-PAA

The moisture-free CSM was polymerized with AA by the free radical polymerization method reported previously,[24] in which KPS generated free radicals of CSM and MBA crosslinked CSM

with AA. Different concentrations of CSM, AA, KPS, and MBA were used to synthesize the copolymer (Table 1), which was used in nine different formulations. Due to its high swelling, C-6 was prepared by stirring an aqueous suspension of CSM (1.5 g per 100 g) at 70 °C for 15 min to obtain a sticky transparent material before adding KPS (0.5 g per 100 g) to generate free radicals of CSM. The reaction mixture (solution 1) was then allowed to cool at room temperature. After that, the cross-linker MBA (0.6 g per 100 g) was solubilized in AA (20 g per 100 g) at room temperature (solution 2). Solutions 1 and 2 were mixed and stirred for 30 min at room temperature and then shifted to test tubes and heated in an electrical water bath at 80 °C until the appearance of a transparent copolymer/hydrogel (CSM-*g*-PAA). After 6 h, test tubes containing the CSM-*g*-PAA hydrogel were cooled at room temperature and then the hydrogel was cut into 5 to 8 mm-sized discs after washing with DW. The discs were kept in an air-tight vessel and washed with a mixture of ethanol and DW (70 : 30%, v/v) until the neutralization of the pH of the washing medium was achieved. The washed discs were spread on a glass tray in a vacuum oven, where they were dried at 60 °C until the attainment of constant weight. Using the same protocol, eight more formulations of CSM-*g*-PAA were synthesized by changing the ratios of CSM, AA, and MBA to investigate the effect of increasing the concentrations of CSM, AA, and MBA in the reaction mixture on the swelling capacity (g g^{-1}), sol–gel fraction (%), porosity (%), and nicorandil loading (mg g^{-1}) and release (%).

2.5. pH-responsive swelling studies of CSM-g-PAA

The pH-responsive swelling properties of all formulations of CSM-*g*-PAA were studied in the buffers of pH 1.2, 6.8, and 7.4 using the gravimetric method, as reported in ref. 25. The pre-weighed and moisture-free CSM-*g*-PAA hydrogel discs were immersed in the buffers of pH 1.2, 6.8, and 7.4 at room temperature. The surplus water on the swelled CSM-*g*-PAA discs was removed with filter paper. The weight of swelled CSM-*g*-PAA discs was noted after regular time intervals of 0, 0.5, 1, 1.5, 2, 3, 4, 6, 8, 10, 12, 16, 24, 36, 48, and 72 h. The dynamic swelling of all the nine formulations of CSM-*g*-PAA was calculated using eqn (1).

$$Q = \frac{W_s}{W_d} \tag{1}$$

where W_d and W_s are the weights (g) of dry and swollen CSM-*g*-PAA discs at $t = 0$ and any time t, respectively.

The swollen CSM-*g*-PAA discs in every swollen medium were allowed to further swell in their respective medium until no more change in the swollen state of CSM-*g*-PAA was observed, *i.e.*, for 72 h, and the equilibrium swelling (%ES) of CSM-*g*-PAA was calculated using eqn (2).

$$\%\ \mathrm{ES} = \frac{(M_{eq} - M_0)}{M_{eq}} \times 100 \tag{2}$$

where M_{eq} is the weight (g) of swollen CSM-*g*-PAA at equilibrium and M_0 is the initial mass of CSM-*g*-PAA discs in dry form at $t = 0$.

Table 1 Amounts of CSM (g per 100 g), AA (g per 100 g), KPS (g per 100 g), and MBA (g per 100 g) for synthesizing the copolymer CSM-*g*-PAA

Copolymer	CSM	AA	MBA	KPS
C-1	0.5	15	0.6	0.5
C-2	1.0	15	0.6	0.5
C-3	1.5	15	0.6	0.5
C-4	1.5	12.5	0.6	0.5
C-5	1.5	17.5	0.6	0.5
C-6	1.5	20	0.6	0.5
C-7	1.5	15	0.8	0.5
C-8	1.5	15	1.0	0.5
C-9	1.5	15	1.2	0.5

2.6. Swelling kinetics of CSM-g-PAA

The water penetration rate of CSM-*g*-PAA was determined using the second-order swelling kinetics equation (eqn (5)). For this purpose, the normalized degree of swelling (Q_t) and normalized equilibrium degree of swelling (Q_e) were determined using eqn (3) and (4), respectively. The values of Q_t and Q_e were used to investigate second-order swelling kinetics (eqn (5)).

$$Q_t = \frac{W_1 - W_2}{W_2} = \frac{W_t}{W_2} \tag{3}$$

$$Q_e = \frac{W_\infty - W_2}{W_2} = \frac{W_e}{W_2} \tag{4}$$

$$\frac{t}{Q_t} = \frac{t}{Q_e} + \frac{1}{kQ_e^2} \tag{5}$$

where W_1, W_2, W_∞, W_t, and W_e are the weight of CSM-*g*-PAA in swollen form after time "t", the initial dry weight at "$t = 0$", the swollen weight at "$t = \infty$", the weight of penetrated water at time "t", and the weight of retained water at "$t = \infty$".

In second-order kinetics, the plot between $\frac{t}{Q_t}$ and t gives a straight line with a slope of $\frac{1}{Q_e}$ and an intercept of $\frac{1}{kQ_e^2}$, which depicts that the mechanism of swelling depends on the relaxation of the polymeric chains.[26]

2.7. pH-responsive on and off switching

Because of maximum swelling, CSM-*g*-PAA (C-6) was selected to evaluate pH-responsive swelling and de-swelling (on and off switching) in the buffers of pH 7.4 and 1.2 alternately using the gravimetric method. A pre-weighed dry disc of CSM-*g*-PAA was immersed in the buffer of pH 7.4 (50 mL) and allowed to swell for 72 h. The same fully swollen disc of CSM-*g*-PAA was transferred to the buffer of pH 1.2 (50 mL) for de-swelling for 30 min. Three cycles of swelling and de-swelling of CSM-*g*-PAA were performed to explore the reproducibility.

2.8. Measurement of sol and gel fractions

The sol is the unreacted and the gel is the reacted fraction of the CSM in CSM-*g*-PAA. Both fractions are vital for estimating the extent of grafting of AA onto the CSM backbone as reported in ref. 27. The un-washed CSM-*g*-PAA discs of every formulation were immersed in a mixture of solvent, *i.e.*, ethanol: DW (70 : 30%, v/v), until constant pH was achieved at room

temperature. Later, the CSM-*g*-PAA discs were removed from the solvent mixture, cleaned with spongy paper, and dried in the vacuum oven at 60 °C until uniform sized discs with uniform weight were obtained. Eqn (6) was applied to the experimental data to determine the percent gel fraction and eqn (7) was used to measure the percent sol fraction.

$$\%\ \text{Gel fraction} = \frac{W_\text{i} - W_\text{f}}{W_\text{i}} \times 100 \quad (6)$$

$$\%\ \text{Sol fraction} = 100 - \text{Gel fraction} \quad (7)$$

where W_i is the initial weight (g) of dry CSM-*g*-PAA and W_f is the final weight of CSM-*g*-PAA after soaking in the mixture of ethanol and DW.

2.9. Measurement of porosity

The solvent displacement method as reported in ref. 28 was used to quantify the porosity of CSM-*g*-PAA. Briefly, pre-weighed discs of CSM-*g*-PAA were dipped in the beakers containing ethanol at room temperature for 24 h. After that, CSM-*g*-PAA discs were removed from the beakers and weighed. The volume of the CSM-*g*-PAA discs was determined using a graduated cylinder. Eqn (8) was used to measure the porosity of CSM-*g*-PAA discs.

$$\%\ \text{Porosity} = \frac{M_\text{f} - M_\text{i}}{\rho V} \times 100 \quad (8)$$

where M_i is the initial weight (g) of CSM-*g*-PAA discs, M_f is the final weight (g) of CSM-*g*-PAA discs after soaking in the ethanol, ρ is the density (g cm^{-3}) of ethanol and V is the volume (cm^3) of CSM-*g*-PAA discs after immersing in ethanol.

2.10. Loading of nicorandil onto CSM-*g*-PAA discs

To judge the ability of CSM-*g*-PAA to act as a pH-responsive sustained release drug delivery carrier, nicorandil as a model drug was loaded onto synthesized CSM-*g*-PAA samples using a gravimetric method.[29] Nicorandil (1% w/v) solution in the buffer (pH 7.4) was used to soak dried discs of CSM-*g*-PAA for 24 h at room temperature. The nicorandil loaded-CSM-*g*-PAA (Nic-CSM-*g*-PAA) discs in the solution were washed with DW and cleaned with filter paper to remove the contents of nicorandil from the surface. The Nic-CSM-*g*-PAA discs were then spread on the glass tray and dried in the oven at 60 °C until they attained constant weight. The amount of nicorandil loaded onto CSM-*g*-PAA discs was determined using eqn (9).

$$\text{Amount of nicorandil loaded onto discs} = W_2 - W_1 \quad (9)$$

where W_2 is the weight (g) of the dried Nic-CSM-*g*-PAA discs and W_1 is the weight (g) of the dried CSM-*g*-PAA discs.

2.11. *In vitro* release studies of nicorandil from Nic-CSM-*g*-PAA

The dissolution studies were performed on the USP Dissolution Apparatus II at 37 ± 0.5 °C and 50 rpm to investigate the potential of CSM-*g*-PAA as a pH-responsive material for *in vitro* nicorandil release from all the formulations of Nic-CSM-*g*-PAA. The nicorandil release from Nic-CSM-*g*-PAA discs was studied by the time-dependent method to assess the effect of concentrations of CSM, AA, and MBA and pH of the dissolution medium. This is because it is not possible to investigate the kinetics and drug release mechanism without studying the drug release from the hydrogel using the time-dependent method. To determine the kinetics and mechanism of nicorandil release from Nic-CSM-*g*-PAA discs, the time-dependent release studies were conducted for 24 h in the buffers of pH 1.2 (900 mL), 6.8 (900 mL), and 7.4 (900 mL). The discs were immersed in the corresponding buffers and 10 mL of the sample from dissolution vessels was taken after a pre-decided time interval, *i.e.*, at 0, 0.5, 1, 2, 3, 4, 8, 12, 16, 20, and 24 h using a graduated pipette. The amount of dissolution media in the dissolution vessels was restored by adding fresh buffers. Before running the sample on the UV-vis spectrophotometer at 274 nm to record absorbance, the sample was filtered and diluted. The amount of nicorandil released from discs was determined using eqn (10).

$$\%\ \text{Nicorandil release} = \frac{F_t}{F_\text{loaded}} \times 100 \quad (10)$$

where F_t is the quantity of nicorandil released from Nic-CSM-*g*-PAA discs after any time t and F_loaded is the total amount of nicorandil loaded onto CSM-*g*-PAA discs after 24 h.

2.12. Nicorandil-release kinetics and mechanism

To evaluate the release kinetics and mechanism of nicorandil release from drug-loaded discs, a model-dependent approach was used by applying numerous kinetic models such as zero-order (eqn (11)),[30] first-order (eqn (12)),[31] Higuchi (eqn (13)),[32] Hixon–Crowell (eqn (14)),[33] and Korsmeyer–Peppas models (eqn (15)).[34]

$$Q_t = K_0 t \quad (11)$$

$$\log Q = \log Q_0 - \left(\frac{k_1 t}{2.303}\right) \quad (12)$$

$$Q_0^{\frac{1}{3}} - Q_t^{\frac{1}{3}} = -K_\text{HC} t \quad (13)$$

$$Q_t = -K_\text{H} (t)^{\frac{1}{2}} \quad (14)$$

$$\frac{M_t}{M_\infty} = k_\text{p} t^n \quad (15)$$

where Q_0 and Q_t indicate the initial amount of loaded nicorandil and the amount of nicorandil released from Nic-CSM-*g*-PAA after time t, respectively. K_0, k_1, K_HC, K_H, and k_p are the kinetic constants of zero, first, Hixon–Crowell, Higuchi, and Korsmeyer–Peppas models, respectively. n represents the diffusion exponent. Its value can be 0.45, between 0.45 and 0.89 or >0.89 for Fickian diffusion, non-Fickian diffusion, or super case-II transport, respectively.[34–36] The term $\frac{M_t}{M_\infty}$ is the amount of nicorandil released from Nic-CSM-*g*-PAA at a time "t".

A modified Akaike Information Criterion, *i.e.*, the model selection criterion (MSC) (eqn (16)), was also applied to know about the best fit of the kinetic model to nicorandil release data from Nic-CSM-*g*-PAA.[37] The cases where the highest MSC value

will be obtained after fitting the drug release data to different kinetic models revealed the best-fit model.

$$\mathrm{MSC} = \ln\left(\frac{\sum_{i=1}^{n} w_i(Y_{\mathrm{obs}_i} - \bar{Y}_{\mathrm{obs}})^2}{\sum_{i=1}^{n} w_i(Y_{\mathrm{obs}_i} - Y_{\mathrm{cal}_i})^2}\right) - \frac{2p}{n} \qquad (16)$$

where Y_{obs_i}, Y_{cal_i}, and $\bar{Y}_{\mathrm{obs}}$ represent the observed value of the ith data point, the calculated value of the ith data point, and the mean of observed data points, respectively. w_i, p, and n denote the optional weight factor, the number of parameters, and the number of data points, respectively.

2.13. Statistical analysis

The tests regarding swelling, on–off switching, sol–gel fraction, porosity, nicorandil loading, and nicorandil release were conducted in triplicates and the average values along with standard deviation (± SD) were noted and reported herein.

3. Results and discussion

3.1. Synthesis of CSM-*g*-PAA

Using the free radical polymerization reaction, a series of novel hydrogels based on CSM and AA were synthesized. KPS was used as an initiator and MBA as a cross-linker. A total of nine formulations of CSM-*g*-PAA (C-1 to C-9) were synthesized by changing the concentrations of CSM, AA, and MBA in the reaction mixture. The concentration of KPS was kept constant at 0.5% in all the formulations. The grafting percentage (%G) of AA onto a copolymer hydrogel (CSM-*g*-PAA) was calculated using the equation given below (eqn 17) and it was found to be 80% for an optimized formulation, *i.e.*, C-6.

$$\%G = \frac{W_g - W_o}{W_o} \times 100 \qquad (17)$$

where W_g and W_o denote the weights of the grafted polymer (CSM-*g*-PAA) after modification and the monomer (AA) used for polymerization, respectively.

The influence of variable concentrations of CSM, AA, and MBA on the swelling (dynamic and equilibrium) behavior, sol–gel fraction, porosity, and drug release was evaluated. The formulation C-6 was selected for analysis purposes because of its high swelling and pH sensitivity and further studies were performed on this sample. A plausible reaction scheme representing the illustrated structure of CSM-*g*-PAA is presented below (Fig. 1).

3.2. Characterization

A prominent peak at 2924 cm^{-1} appeared due to the presence of hydroxyl (–OH) functionality in sugar units, which overlapped with the –CH and $–CH_2$ signals of the CSM. Similarly, two peaks at 1678 cm^{-1} belonging to the carbonyl (–C═O) functional group of carboxylic (–COOH) revealed uronic acid-type moieties in the CSM. In addition, a broad band at 1150–900 cm^{-1} is due to the presence of the C–O–C functional group, confirming the glycosidic linkage in the polymeric chains of the CSM.[38] The FTIR spectrum of CSM-*g*-PAA (Fig. 2) revealed the appearance of a new signal at 1721 cm^{-1} due to the presence of ester linkage and hence indicated the successful formation of CSM-*g*-PAA through free radical polymerization of the CSM with AA.[39]

The solid-state CP/MAS ^{13}CNMR spectrum of CSM-*g*-PAA is presented in Fig. 3. It is obvious that, after polymerization of the CSM with AA, the CSM displayed –C═O signals at 176.72 ppm, whereas overlapped signals for $–CH_2$ and –CH appeared at 40.68 ppm. Although signals showing polysaccharide regions are often difficult to detect in the NMR spectrum of CSM-*g*-PAA, only signals of C2 and C6 of the sugars are observable in spectrum due to a higher proportion of AA in CSM-*g*-PAA. The study of peers also revealed similar findings.[27,28,40]

SEM images revealed the surface morphology and topography of CSM-*g*-PAA (Fig. 4). SEM disclosed the porous nature of CSM-*g*-PAA and interconnected channels that might be responsible for the absorption of large amounts of water or buffers in

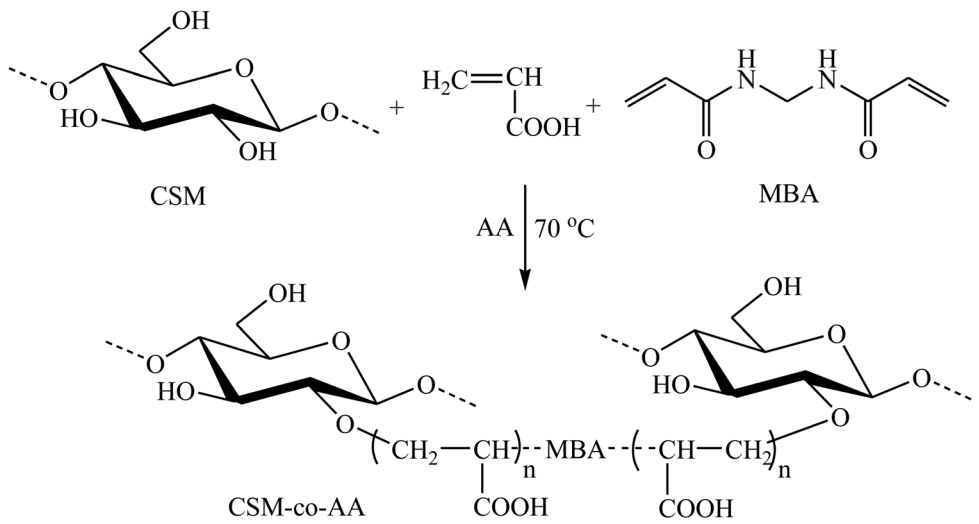

Fig. 1 Hypothetical reaction scheme representing the illustrated structure of the CSM and the AA-based graft copolymer hydrogel (CSM-*g*-PAA).

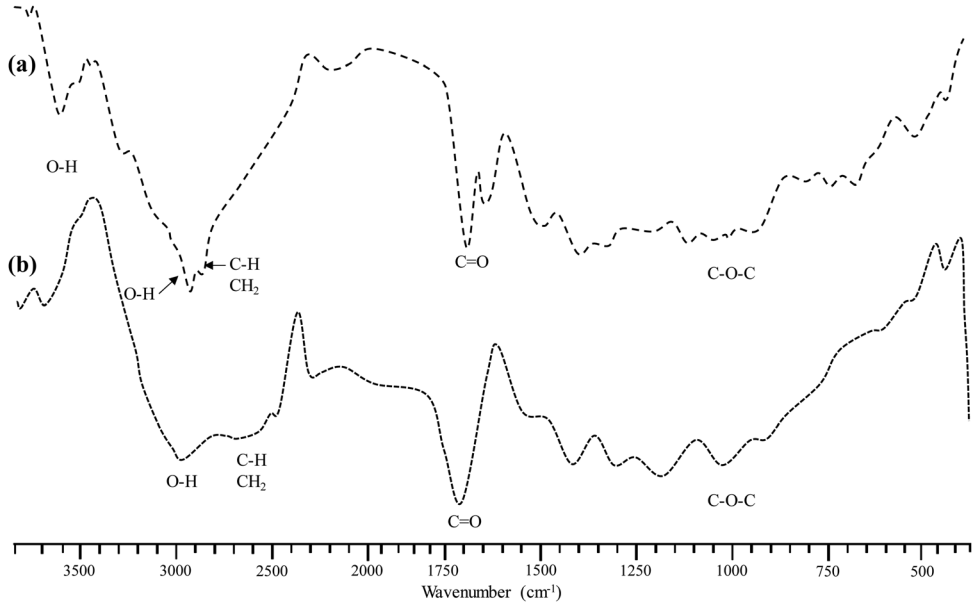

Fig. 2 FTIR spectra of (a) CSM and (b) CSM-*g*-PAA.

the polymeric network of the synthesized hydrogel. The interconnected channels are essential for swelling, on and off switching, nicorandil loading, and nicorandil release from Nic-CSM-*g*-PAA formulations.

3.3. Swelling behavior of CSM-*g*-PAA

3.3.1. Effect of polymer concentration. Polymer (CSM) ratios were varied from 0.5 to 1.5% for CSM-*g*-PAA synthesis while maintaining constant concentrations of AA (15%), MBA (0.6%), and KPS (0.5%) to investigate the effect of CSM concentration on the equilibrium swelling properties of CSM-*g*-PAA. The swelling of CSM-*g*-PAA increased from 1.81 to 1.91 g g^{-1} at pH 1.2, 16.13 to 21.51 g g^{-1} at pH 6.8, and 18.51 to 23.63 g g^{-1} at pH 7.4 upon increasing CSM concentration from 0.5 to 1.5%. The swelling was reduced upon further increasing the concentration of CSM by over 1.5% due to the increase in the cross-linking density of CSM-*g*-PAA. The order of swelling of CSM-*g*-PAA was C-1 < C-2 < C-3 (Fig. 5a) in all the swelling media (pH 1.2, 6.8, and 7.4).[40] Another possibility of lower swelling at 1.5% CSM concentration might include an increment in reaction mixture viscosity imparting steric hindrance to ionic groups of the CSM and inhibiting the free flow of water molecules. Due to greater swelling, it was decided that the optimal CSM (polymer) concentration for further experimental work was 1.5%.

3.3.2. Effect of monomer concentration. By varying the concentration of monomer (AA) from 12.5 to 20% at an optimal concentration of CSM (1.5%), MBA (0.6%), and KPS (0.5%), the influence of monomer concentration on the equilibrium swelling index of CSM-*g*-PAA was studied. Upon increasing the concentration of AA, swelling of CSM-*g*-PAA increases until it reaches an ideal concentration (20%) and then tends to decline. C4 < C5 < C6 was the order of swelling at pH 6.8 and 7.4 (Fig. 5b). However, at pH 1.2 opposite order was seen (Fig. 5b). With the increase of AA amount, the number of –COOH groups and swelling of CSM-*g*-PAA increase due to rise in the concentration gradient of counter ions throughout the polymeric network and osmotic

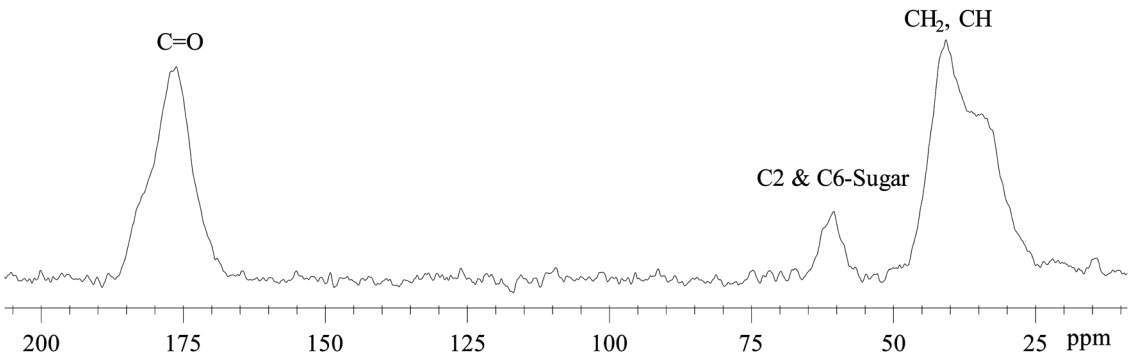

Fig. 3 Solid-state CP/MAS ^{13}CNMR spectrum of CSM-*g*-PAA.

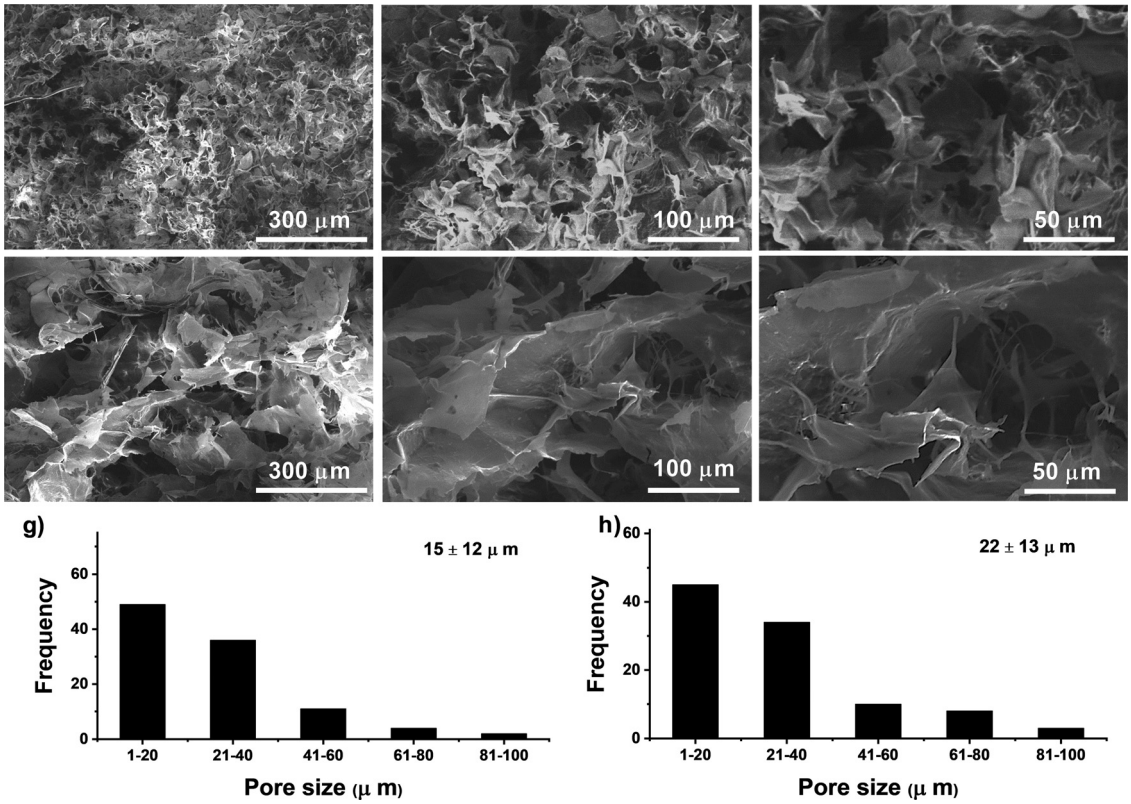

Fig. 4 SEM micrographs of CSM-*g*-PAA at different magnifications: (a) and (b) transverse sections, (c) and (d) longitudinal sections, and (e) and (f) histograms.

pressure applied by the counter ions of AA. Additionally, because AA has a pK_a value of about 4.2 at pH = 5, the –COOH groups of AA become less ionized and CSM-*g*-PAA swells with low swelling capacity, whereas at higher pH levels (>5), the –COOH groups of AA become progressively ionized and CSM-*g*-PAA swelled with high swelling capacity.[40] The availability of –COOH groups for ionization rises as AA concentration in CSM-*g*-PAA rises because it may create electrostatic repulsion of –COOH groups and relax twisted molecules. The hydrophilicity and pH sensitivity of CSM-*g*-PAA increase as a consequence and swelling is also increased.[28] However, upon further increase of AA concentration (>20%), there should be a higher probability that AA will homo-polymerize and create a dense hydrogel network leading to a decrease in the swelling.[27]

3.3.3. Effect of cross-linker concentration. By maintaining constant concentrations of CSM (1.5%), AA (20%), and KPS (0.5%), the concentration of MBA was changed from 0.6 to 1.2% to investigate the impact of MBA concentration on the equilibrium swelling of CSM-*g*-PAA. High swelling was attained at a lower concentration of MBA. MBA concentration improved the cross-linking density (Fig. 5c), resulting in a more compact, rigid, and stable framework for these molecules.[41] Furthermore, physical entanglement between hydrogel chains increased due to the high concentration of cross-linker, which caused the polymer to become strongly cross-linked and far less acidic. As a consequence, –COOH groups of CSM-*g*-PAA surround the polymer chain reducing its mobility, delaying the ionization process, and increasing hydrophobicity.[28] Hence, upon increasing the concentration of the MBA cross-linker, the swelling was significantly reduced. Therefore, the optimal concentration of MBA was 0.6% for the synthesis of CSM-*g*-PAA.

3.3.4. Effect of pH. Due to high swelling, the CSM-*g*-PAA formulation C-6 was chosen to estimate the effect of pH (pH 1.2, 6.8, and 7.4) on dynamic swelling patterns at room temperature (37 °C). At pH 7.4, the swelling index was high; however, minor swelling was noted at pH 1.2 (Fig. 5d). The swelling order was noted to be pH 1.2 < pH 6.8 < pH 7.4. The majority of –COOH groups in CSM-*g*-PAA networks are protonated, which eliminates anion–anion repulsions of the carboxylate anion ($–COO^-$), causing less swelling in the acidic environment.[41] The –COOH groups of CSM-*g*-PAA began to ionize into $–COO^-$ and produced electrostatic ($–COO^-$ and $–COO^-$) repulsions across CSM chains when the pH of the swelling medium rose from pH 1.2 to pH 6.8 and 7.4.[27]

3.3.5. Swelling kinetics. To study the swelling kinetics of CSM-*g*-PAA, swelling data collected from the C-6 formulation were fitted to equations of several kinetic models. Swelling data closely matched with second-order kinetics (Fig. 6a). This showed that the relaxation-controlled mechanism was responsible for CSM-*g*-PAA swelling.

3.3.6. On and off switching. Formulation C-6 was selected to study the on and off-switching characteristics of CSM-*g*-PAA at pH 7.4 and 1.2. Fig. 6b demonstrates the on and off switching behavior of CSM-*g*-PAA. The swelling process was allowed to proceed for 48 h since CSM-*g*-PAA swelled slowly at pH 7.4.

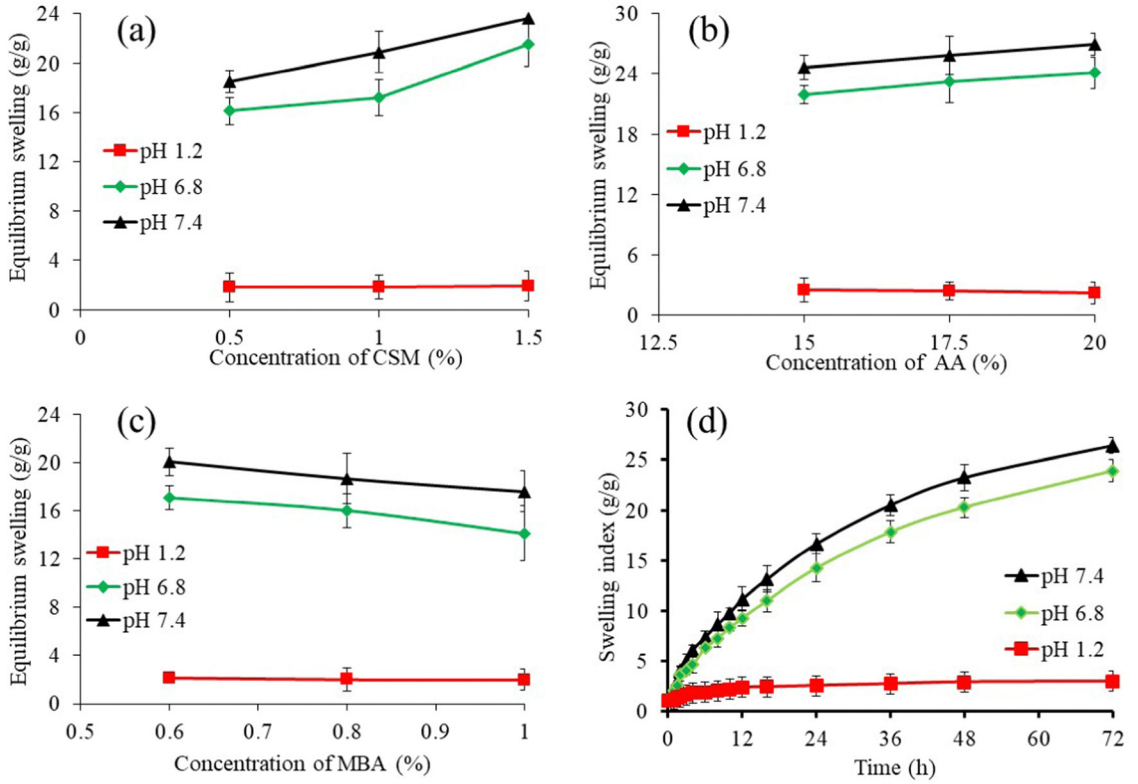

Fig. 5 Equilibrium swelling index of CSM-*g*-PAA showing the effect of concentrations of CSM (a), AA (b), and MBA (c) after 72 h and pH-responsive dynamic swelling of CSM-*g*-PAA (formulation C-6) (d) after 72 h.

Then, CSM-*g*-PAA (swollen form) was switched to pH 1.2 for de-swelling. In about 30 min, CSM-*g*-PAA was de-swelled completely. CSM-*g*-PAA swelling and de-swelling behaviors may be related to the switching between ionized (–COO-) and un-ionized (–COOH) forms of –COOH groups. On and off switching swelling procedures were carried out to record three consecutive cycles and essentially identical results were obtained, demonstrating pH responsiveness and repeatability of data.

3.4. Measurement of the sol–gel fraction

To calculate the quantities of soluble, uncross-linked, and insoluble cross-linked components in the gel structures of CSM-*g*-PAA, experiments related to the measurement of the sol–gel fraction were carried out. The sol–gel fraction was determined from the increase in gel contents in percentage (%) with the increase in the concentrations of CSM, AA, and MBA (Fig. 7a). CSM concentration improved along with the number of free radicals needed to cause AA to polymerize. Similar to this, increasing amounts of AA produced an an increasing number of free radicals in the reaction mixture, enabling efficient cross-linking of the CSM with AA. Furthermore, a thick and extremely cross-linked material was synthesized because of a greater amount of MBA, which further improved the process of cross-linking between CSM and AA.[28] On the other hand, the sol

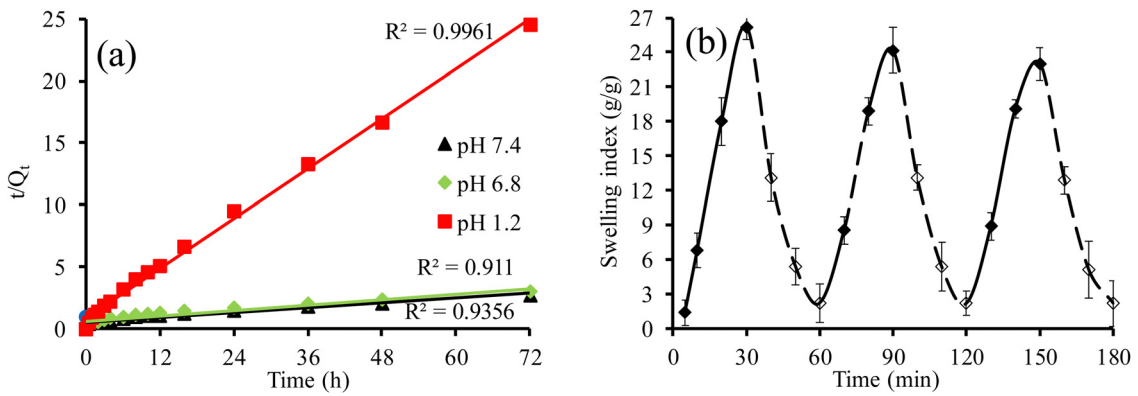

Fig. 6 Swelling kinetics of CSM-*g*-PAA showing the second-order swelling of CSM-*g*-PAA (formulation C-6) (a) and the on and off switching behavior of CSM-*g*-PAA (formulation C-6) at pH 7.4 and 1.2 (b).

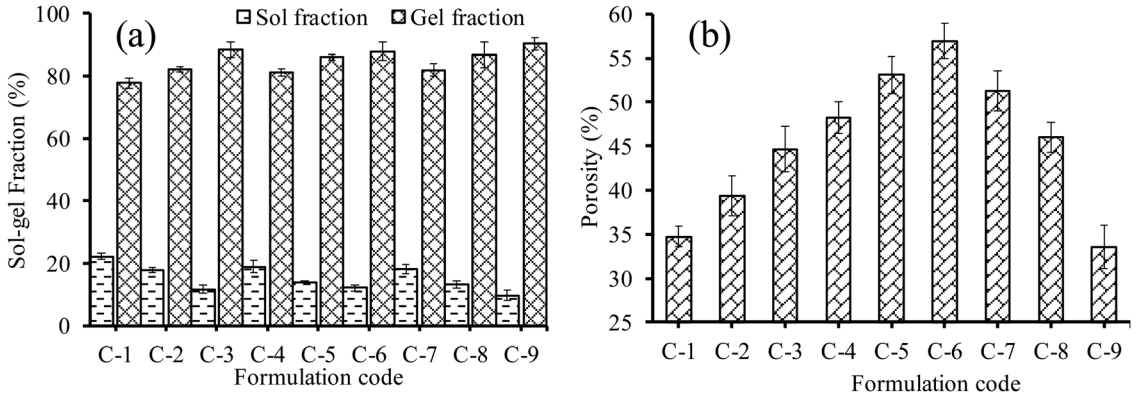

Fig. 7 Determination of the sol–gel fraction (a) and porosity (b) of CSM-*g*-PAA.

fraction (%) exhibited an inverse tendency, meaning that as the concentrations of CSM, AA, and MBA increased, so did the sol fraction (%). Furthermore, >10% of sol fraction in CSM-*g*-PAA (all formulations) was found, which indicated the presence of an insignificant amount of unreactive ingredients in it. On the other hand, <90% of the gel fraction was noted, which revealed the presence of a significant amount of reactive ingredients in CSM-*g*-PAA. Hence, this finding assured the removal of all unreactive components from CSM-*g*-PAA using 70% ethanol (Fig. 7a).[27]

3.5. Determination of porosity

While evaluating the feasibility of any hydrogel as a pharmaceutical excipient in drug delivery applications, porosity measurement is a key factor. Porosity measurements were often used to investigate how polymers, monomers, and cross-linkers affect the size of hydrogel pores. A hydrogel's capacity to absorb water from the swelling medium will increase with increasing pore size and lead to an increase in swelling.[24] Hence, to investigate the effect of CSM, AA, and MBA on the pore size of hydrogels, measurements of the porosity of CSM-*g*-PAA were made. Fig. 7b indicates the obtained results. It was discovered that the porosity increased by raising the amounts of both CSM and AA. This may be because more –OH groups, viscosity, and air entrapment result from higher CSM and AA concentrations. Hydrogen bonding was made stronger by the increase in –OH groups. Because of the increase in cross-linking density and physical interaction between polymers and monomers, an opposite effect was seen when the concentration of MBA was increased.[28]

3.6. Drug loading

The model drug nicorandil was successfully loaded onto all formulations of CSM-*g*-PAA. It was found that the loading of the drug was directly related to the swelling indices of CSM-*g*-PAA.[27] This means that nicorandil was absorbed from its solution in large amounts by CSM-*g*-PAA formulations that had a greater swelling index and *vice versa*. Additionally, it was shown that nicorandil loading onto CSM-*g*-PAA increased when CSM and AA concentrations were high and reduced when MBA concentrations were low (Table 2). Increased swelling of CSM-*g*-PAA with higher concentrations of CSM and AA and reduced swelling with higher concentrations of MBA may be the contributing factors to these changes. Additionally, reduced swelling is linked to increased cross-linking density, which in turn decreases the flexibility of the polymeric structure, preventing nicorandil from moving from the drug solution into CSM-*g*-PAA. Hence, nicorandil's loading was decreased.

3.7. *In vitro* drug release

The drug (nicorandil) release from Nic-CSM-*g*-PAA was found to be strongly directly related to the amounts of CSM. Upon increasing the amounts of CSM from 0.5% to 1.0% and 1.5%, the nicorandil release was noted to be 6.21, 7.9, and 8.76% in buffer of pH 1.2; 62.7, 65.22, and 69.77% in buffer of pH 6.8; and 75.89, 77.98, and 81.14% in buffer of pH 7.4, respectively, after 24 h (Fig. 8a). This is because upon increasing the concentration of CSM, the swelling indices of CSM-*g*-PAA (formulations C-1, C-2, and C-3) were found to increase.[24] This means that the nicorandil release from CSM-*g*-PAA is directly related to the swelling indices.

With the increase in the concentration of monomer (AA) from 15 to 20.0%, the nicorandil release was also increased and noted to be 6.11, 5.7, and 5.13% in buffer of pH 1.2; 74.51, 78.77, and 4.13% in buffer of pH 6.8; and 83.12, 88.98, and 95.31% in buffer of pH 7.4, respectively, after 24 h (Fig. 8b). This is because by increasing the amount of AA the swelling of CSM-*g*-PAA had been increased.[28]

The release behavior of nicorandil from Nic-CSM-*g*-PAA was also investigated by changing the concentration of MBA from 0.6 to 1.2% and it appeared to be directly dependent on the concentration of MBA in the formulation design of CSM-*g*-PAA.[40] Quantitatively, the nicorandil release was found to be 5.07, 4.91, and 4.53% in the buffer of pH 1.2; 60.65, 56.77, and 51.34% in the buffer of pH 6.8; and 71.9, 67.9, and 63.21% in the buffer of pH 7.4, respectively after 24 h (Fig. 8c).

The potential of CSM-*g*-PAA as a pH-responsive controlled release DDS was evaluated at pH 1.2, 6.8, and 7.4 (at 37 °C for 24 h). It was found that nicorandil release was closely connected to the dissolving media's pH and swelling indices of CSM-*g*-PAA. At pH 1.2, nicorandil release was found to be 8.73% after 24 h. However, when the pH of the dissolving medium was changed to pH 6.8 (84.67%) and pH 7.4 (95.77%), a high amount

Table 2 Drug loading onto CSM-*g*-PAA

Formulation	Nicorandil loaded amount (mg)
C-1	110
C-2	122
C-3	127
C-4	134
C-5	142
C-6	147
C-7	105
C-8	102
C-9	97

of nicorandil release as mentioned in the parentheses was found. The trend of nicorandil release was pH 7.4 > pH 6.8 > pH 1.2. This may be because CSM-*g*-PAA swells significantly well at pH 7.4 (Fig. 8d).

3.8. Nicorandil-release mechanism

Identifying the mass transport mechanism involved in drug release is necessary to provide a DDS with predictable release behavior. By fitting release data to several kinetic models, the mechanism of nicorandil release from Nic-CSM-*g*-PAA was investigated (Table 3). Values of R^2 were used to measure the "goodness of fit" of kinetic models to release data, and values of n were used to calculate the drug release mechanism. Because R^2 values for all the formulations of Nic-CSM-*g*-PAA were high once the nicorandil release data from Nic-CSM-*g*-PAA were fitted to the Korsmeyer–Peppas model; therefore, it was discovered that release data were fitted well to the Korsmeyer–Peppas model (0.9896 at pH 1.2, 0.9882 at pH 6.8, and 0.9855 at pH 7.4) in a best manner. Additionally, the values of n were found to be 0.6140 at pH 1.2, 0.5270 at pH 6.8, and 0.4880 at pH 7.4, demonstrating non-Fickian transport for nicorandil release.[34,35]

Table 3 Nicorandil release kinetics data from the C-6 formulation of CSM-*g*-PAA

Drug release model		pH 1.2	pH 6.8	pH 7.4
Zero-order	R^2	0.9651	0.9761	0.9686
	K_0	0.4230	8.9980	11.1740
	MSC	1.6524	2.2892	1.7792
First-order	R^2	0.9678	0.9944	0.9960
	K_1	0.004	0.0970	0.144
	MSC	1.841	3.4460	3.8229
Higuchi	R^2	0.9556	0.9747	0.9856
	K_H	1.6910	18.0150	21.5220
	MSC	2.9474	3.4358	3.2810
Korsmeyer–Peppas	R^2	0.9896	0.9882	0.9855
	K_{KP}	1.2610	16.8210	22.1470
	n	0.6140	0.5270	0.4880
	MSC	3.4835	3.3335	3.1441
Hixson–Crowell	R^2	0.9669	0.9876	0.9409
	K_{HC}	0.0010	0.0270	0.0400
	MSC	1.7158	2.4703	2.6465

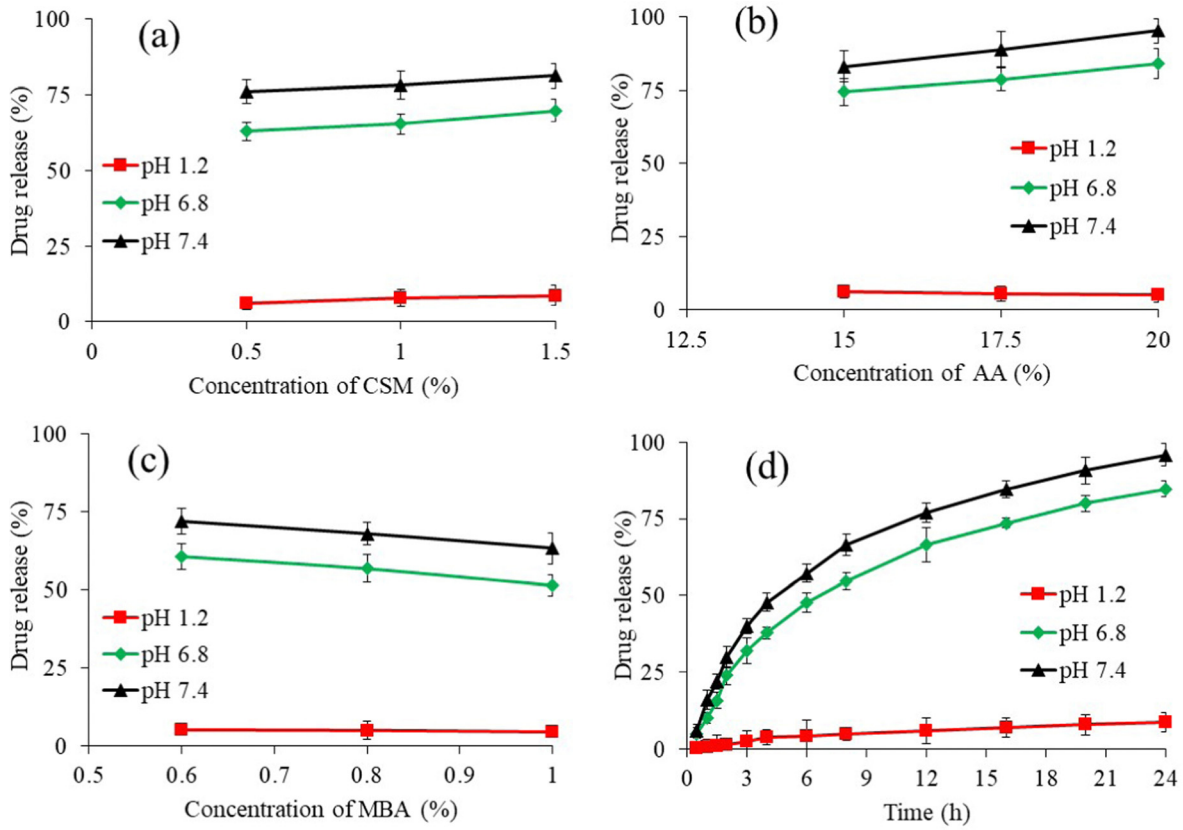

Fig. 8 Nicorandil release from Nic-CSM-*g*-PAA showing the effect of CSM (a), AA (b), MBA (c), and pH (d) after 24 h.

4. Conclusion

The CSM mucilage (a polysaccharide, glucoxylan) obtained from chia seeds was used to develop an acrylic acid (AA) based copolymer hydrogel (CSM-*g*-PAA), which was effectively used as a new excipient of natural origin for producing smart drug delivery systems. A series of nine different formulations (C-1 to C-9) of the copolymer hydrogel (CSM-*g*-PAA) were successfully developed, encapsulated with nicorandil, and thoroughly characterized by FTIR, solid-state CP/MAS ^{13}C NMR, and SEM for the possible treatment of colon-specific diseases. Based on the physical appearance, highest swelling capacity, nicorandil loading and release capacity, and pH dependency, the formulation C-6 (CSM = 1.5 g per 100 g, AA = 20 g per 100 g, MBA = 0.6 g per 100 g, and KPS = 0.6 g per 100 g) appeared to be the ideal formulation. As the release of nicorandil from the copolymer hydrogel (Nic-CSM-*g*-PAA) was greater at simulated intestinal pH rather than at acidic pH, such hydrogel systems can be used to increase patient compliance by reducing the dose frequency. Conclusively, the Nic-CSM-*g*-PAA hydrogel can effectively be used for the treatment of hypertension and angina, and such a model may be expanded to include other anti-hypertensive drugs used for treating different conditions in the future.

Author contributions

Maria Khatoon: investigation, writing – original draft; Arshad Ali: methodology, investigation, writing – original draft; Muhammad Ajaz Hussain: conceptualization, supervision, project administration, writing – reviewing and editing; Muhammad Tahir Haseeb: validation, writing – reviewing and editing; Gulzar Muhammad: formal analysis, data curation; Muhammad Sher: supervision, project administration; Syed Zajif Hussain: formal analysis; Irshad Hussain: formal analysis, resources; and Munawar Iqbal: data curation, validation.

Data availability

No data were used for the research described in the article.

Conflicts of interest

There are no conflicts to declare.

Acknowledgements

We acknowledge Dr Irfan Azhar, the Southern University of Science and Technology, Shenzhen, China, for the provision of the solid-state CP/MAS ^{13}C NMR spectrum of CSM-*g*-PAA.

References

1 G. Goksen, D. Demir, K. Dhama, M. Kumar, P. Shao, F. Xie, N. Echegaray and J. M. Lorenzo, Mucilage polysaccharide as a plant secretion: Potential trends in food and biomedical applications, *Int. J. Biol. Macromol.*, 2023, **230**, 123146.
2 S. Beikzadeh, A. Khezerlou, S. M. Jafari, Z. Pilevar and A. M. Mortazavian, Seed mucilages as the functional ingredients for biodegradable films and edible coatings in the food industry, *Adv. Colloid Interface Sci.*, 2020, **280**, 102164.
3 M. A. Abd El-Ghaffar, M. S. Hashem, M. K. El-Awady and A. M. Rabie, pH-sensitive sodium alginate hydrogels for riboflavin controlled release, *Carbohydr. Polym.*, 2012, **20**, 667–675.
4 M. S. Hashem, H. S. Magar, A. M. Fahim and R. A. Sobh, Antimicrobial, antioxidant, mechanistic, docking simulation, and electrochemical studies for grafting polymerization of novel sulphonated gelatin derived from chicken feet, *Mater. Chem. Phys.*, 2023, **310**, 128474.
5 M. S. Hashem, R. A. Sobh, A. M. Fahim and G. H. Elsayed, Alginate sulfonamide hydrogel beads for 5-fluorouracil delivery: antitumor activity, cytotoxicity assessment, and theoretical investigation, *Int. J. Biol. Macromol.*, 2024, **282**, 136573.
6 M. S. Hashem, A. M. Fahim and F. M. Helaly, Designing a green poly (β-amino ester) for the delivery of nicotinamide drugs with biological activities and conducting a DFT investigation, *RSC Adv.*, 2024, **14**, 5499–5513.
7 M. S. Hashem and H. S. Magar, Creative synthesis of pH-dependent nanoporous pectic acid grafted with acrylamide and acrylic acid copolymer as an ultrasensitive and selective riboflavin electrochemical sensor in real samples, *Int. J. Biol. Macromol.*, 2024, **280**, 136022.
8 S. Fazli, S. Hezari and A. Olad, Preparation of hydrogels based on okra pods/chia seeds mucilage for drug delivery application, *Polym. Bull.*, 2024, 1–24.
9 M. Grancieri, H. S. D. Martino and E. Gonzalez de Mejia, Chia Seed (*Salvia hispanica* L.) as a source of proteins and bioactive peptides with health benefits: A review, *Compr. Rev. Food Sci. Food Saf.*, 2019, **18**, 480–499.
10 W. Khalid, M. S. Arshad, A. Aziz, M. A. Rahim, T. B. Qaisrani, F. Afzal, A. Ali and M. M. A. N. Ranjha, Chia seeds (*Salvia hispanica* L.): A therapeutic weapon in metabolic disorders, *Food Sci. Nutr.*, 2023, **11**, 3–16.
11 Y. P. Timilsena, R. Adhikari, S. Kasapis and B. Adhikari, Molecular and functional characteristics of purified gum from Australian chia seeds, *Carbohydr. Polym.*, 2016, **136**, 128–136.
12 K. Y. Lin, J. R. Daniel and R. L. Whistler, Structure of chia seed polysaccharide exudate, *Carbohydr. Polym.*, 1994, **23**, 3–18.
13 S. Ribes, N. Peña, A. Fuentes, P. Talens and J. M. Barat, Chia (*Salvia hispanica* L.) seed mucilage as a fat replacer in yogurts: Effect on their nutritional, technological, and sensory properties, *J. Dairy Sci.*, 2021, **104**, 2822–2833.
14 A. Das, Advances in chia seed research, *Adv. Biotechnol. Microbiol.*, 2018, **5**, 5–7.
15 B. E. Campos, T. D. Ruivo, M. R. da Silva Scapim, G. S. Madrona and R. D. C. Bergamasco, Optimization of the mucilage extraction process from chia seeds and

application in ice cream as a stabilizer and emulsifier, *LWT-Food Sci. Technol.*, 2016, **65**, 874–883.
16 R. Ullah, M. Nadeem, A. Khalique, M. Imran, S. Mehmood, A. Javid and J. Hussain, Nutritional and therapeutic perspectives of Chia (*Salvia hispanica* L.): A review, *J. Food Sci. Technol.*, 2016, **53**, 1750–1758.
17 S. Ribes, R. Grau and P. Talens, Use of chia seed mucilage as a texturing agent: Effect on instrumental and sensory properties of texture-modified soups, *Food Hydrocoll.*, 2022, **123**, 107171.
18 M. Dick, T. M. H. Costa, A. Gomaa, M. Subirade, A. Rios and S. H. Flôres, Edible film production from chia seed mucilage: Effect of glycerol concentration on its physicochemical and mechanical properties, *Carbohydr. Polym.*, 2015, **130**, 198–205.
19 I. F. S. Ramos, L. M. Magalhães, C. O. Pessoa, P. M. P. Ferreira, M. S. Rizzo, J. A. Osajima, E. C. Silva-Filho, C. Nunes and F. Raposo, New properties of chia seed mucilage (*Salvia hispanica* L.) and potential application in cosmetic and pharmaceutical products, *Ind. Crops Prod.*, 2021, **171**, 113981.
20 J. E. Elliott, M. Macdonald, J. Nie and C. N. Bowman, Structure and swelling of poly(acrylic acid) hydrogels: Effect of pH, ionic strength, and dilution on the crosslinked polymer structure, *Polymer*, 2004, **45**, 1503–1510.
21 D. Hawthorne, A. Pannala, S. Sandeman and A. Lloyd, Sustained and targeted delivery of hydrophilic drug compounds: A review of existing and novel technologies from bench to bedside, *J. Drug Deliv. Sci. Technol.*, 2022, **78**, 103936.
22 J. Y. Kim, C. W. Park, B. J. Lee, E. S. Park and Y. S. Rhee, Design and evaluation of nicorandil extended-release tablet, *Asian J. Pharm. Sci.*, 2015, **10**, 108–113.
23 M. Khatoon, A. Ali, M. A. Hussain, M. T. Haseeb, M. Sher, O. A. Alsaidan, G. Muhammad, S. Z. Hussain, I. Hussain and S. N. A. Bukhari, A superporous and pH-sensitive hydrogel from *Salvia hispanica* (chia) seeds: stimuli responsiveness, on–off switching, and pharmaceutical applications, *RSC Adv.*, 2024, **14**, 27764–27776.
24 A. Ali, M. T. Haseeb, M. A. Hussain, U. R. Tulain, G. Muhammad and I. Azhar, A pH responsive and superporous biocomposite hydrogel of *Salvia spinosa* polysaccharide-*co*-methacrylic acid for intelligent drug delivery, *RSC Adv.*, 2023, **13**, 4932–4948.
25 H. Yin, P. Song, X. Chen, M. Xiao, L. Tang and H. Huang, Smart pH-sensitive hydrogel based on the pineapple peel-oxidized hydroxyethyl cellulose and the Hericium erinaceus residue carboxymethyl chitosan for use in drug delivery, *Biomacromolecules*, 2023, **23**, 253–264.
26 N. Martínez-Vázquez, R. D. C. Antonio-Cruz, A. Álvarez-Castillo, A. Mendoza-Martinez and A. Morales-Cepeda, Swelling kinetic of hydrogels from methyl cellulose and poly(acrylamide), *Rev. Mex. Ing. Quim.*, 2007, **6**, 337–345.
27 A. Ali, M. A. Hussain, M. T. Haseeb, U. R. Tulain, M. Farid-ul-Haq and T. Tabassum, Synthesis, characterization, and acute toxicity of pH-responsive *Salvia spinosa* mucilage-*co*-acrylic acid hydrogel: A smart excipient for drug release applications, *React. Funct. Polym.*, 2023, **181**, 105466.
28 J. Irfan, A. Ali, M. A. Hussain, M. T. Haseeb, T. G. Alsahli, M. Naeem-ul-Hassan, U. R. Tulain, S. Z. Hussain, I. Hussain and I. Azhar, A superabsorbent and pH-responsive copolymer-hydrogel based on acemannan from Aloe vera (*Aloe barbadensis* M.): A smart material for drug delivery, *Int. J. Biol. Macromol.*, 2024, **270**, 132306.
29 Q. A. Ijaz, N. Abbas, M. S. Arshad, A. Hussain and Z. Javaid, Synthesis and evaluation of pH-dependent polyethylene glycol-*co*-acrylic acid hydrogels for controlled release of venlafaxine HCl, *J. Drug Deliv. Sci. Technol.*, 2018, **43**, 221–232.
30 M. Gibaldi and S. Feldman, Establishment of sink conditions in dissolution rate determinations-theoretical considerations and application to non-disintegrating dosage forms, *J. Pharm. Sci.*, 1967, **56**, 1238–1242.
31 J. G. Wagner, Interpretation of percent dissolved-time plots derived from in-vitro testing of conventional tablets and capsules, *J. Pharm. Sci.*, 1969, **58**, 1253–1257.
32 T. Higuchi, Mechanism of rate of sustained action medication. Theoretical analysis of rate of release of solid drugs dispersed in solid matrices, *J. Pharm. Sci.*, 1963, **52**, 1145–1149.
33 A. W. Hixson and J. H. Crowell, Dependence of reaction velocity upon surface and agitation, *Ind. Eng. Chem.*, 1931, **23**, 1160–1168.
34 R. W. Korsmeyer, R. Gurny, E. Doelker, P. Buri and N. A. Peppas, Mechanisms of solute release from porous hydrophilic polymers, *Int. J. Pharm.*, 1983, **15**, 25–35.
35 P. I. Ritger and N. A. Peppas, A simple equation for description of solute release. II. Fickian and anomalous release from swellable devices, *J. Controlled Release*, 1987, **5**, 37–42.
36 J. Siepmann and N. A. Peppas, Mathematical modeling of controlled drug delivery, *Adv. Drug Delivery Rev.*, 2001, **48**, 137–138.
37 M. S. Iqbal, J. Akbar, M. A. Hussain, S. Saghir and M. Sher, Evaluation of hot-water extracted arabinoxylans from ispaghula seeds as drug carriers, *Carbohydr. Polym.*, 2013, **83**, 1218–1225.
38 M. P. Salgado-Cruz, G. Calderón-Domínguez, J. Chanona-Pérez, R. R. Farrera-Rebollo, J. V. Méndez-Méndez and M. Díaz-Ramírez, Chia (*Salvia hispanica* L.) seed mucilage release characterization. A microstructural and image analysis study, *Ind. Crops Prod.*, 2013, **51**, 453–462.
39 N. Ajaz, I. U. Khan, I. Khalid, R. U. Khan, H. A. Khan, S. Asghar and S. H. Khalid, In vitro and toxicological assessment of dexamethasone sodium phosphate loaded pH-sensitive Pectin-g-poly(AA)/PVP semi interpenetrating network, *Mater. Today Commun.*, 2020, **25**, 101325.
40 M. Farid-ul-Haq, M. A. Hussain, A. Ali, M. T. Haseeb, G. Muhammad and T. Tabassum, A pH-responsive Artemisia vulgaris mucilage-*co*-acrylic acid hydrogel: Synthesis, characterization, controlled drug release, toxicity studies, and MRI, *J. Drug Delivery Sci. Technol.*, 2024, **93**, 105468.
41 H. Ijaz, U. R. Tulain, M. U. Minhas, A. Mahmood, R. M. Sarfraz, A. Erum and Z. Danish, Design and in vitro evaluation of pH-sensitive crosslinked chitosan-grafted acrylic acid copolymer (CS-*co*-AA) for targeted drug delivery, *Int. J. Polym. Mater. Polym. Biomater.*, 2022, **71**, 336–348.